Nano Energy 68 (2020) 104302

Contents lists available at ScienceDirect

Nano Energy

journal homepage: http://www.elsevier.com/locate/nanoen

A "Yin"-"Yang" complementarity strategy for design and fabrication of dual-responsive bimorph actuators

Yong-Lai Zhang [a], Jia-Nan Ma [a], Sen Liu [a], Dong-Dong Han [a,*], Yu-Qing Liu [a], Zhao-Di Chen [a], Jiang-Wei Mao [a], Hong-Bo Sun [b,**]

[a] State Key Laboratory of Integrated Optoelectronics, College of Electronic Science and Engineering, Jilin University, 2699 Qianjin Street, Changchun, 130012, China
[b] State Key Laboratory of Precision Measurement Technology and Instruments, Department of Precision Instrument, Tsinghua University, Haidian, Beijing, 100084, China

ARTICLE INFO

Keywords:
Yin-Yang complementarity
Dual-responsive
Actuators
Bi-directional walking robot
Smart claw array

ABSTRACT

Multi-responsive soft actuators that can convert environmental energies to mechanical works are promising for robotics. However, it currently lacks universal and effective concepts to develop dual-responsive bimorph actuators. In this paper, the concept of "Yin"-"Yang" complementarity, a classical theory in the history of Chinese philosophy, has been adopted for designing dual-responsive actuators. The complement of "Yin" and "Yang" means the bilayers can be inter-constraint as well as being complementary in a dual-responsive actuation. As a proof-of-concept, a composite layer of nano-size graphite (Nano-G) and polyvinylidene fluoride (PVDF) has been combined with graphene oxide (GO), forming a bilayer structure. In response to moisture, GO is positive, meaning "Yang", whereas Nano-G@PVDF is negative, meaning "Yin". On the contrary, under light irradiation, GO is negative; whereas the photothermal Nano-G@PVDF layer is positive. We demonstrated a bi-directional walking robot and a smart claw array for controllable moisture/light manipulation. The "Yin"-"Yang" complementarity strategy provides a universal concept for developing multi-responsive bimorph actuators.

1. Introduction

Soft actuators that can deform in a predictable manner under external stimuli have revealed great potential for cutting-edge applications, including soft robots, micro-electromechanical systems (MEMSs) and human-machine interface systems [1–5]. Importantly, actuators could be considered as one of the most prominent examples that provided state-of-the-art conversion of various environmental energies (*e.g.*, heat, light, gravity and chemicals) to mechanical works [6,7]. A universal concept for developing stimuli responsive actuators is assembling different materials of distinct physical/chemical properties into bilayer or multi-layer structures. Under certain stimuli, the as-generated strain mismatch at the bilayer interface would lead to an obvious and predictable deformation. In this way, bilayer actuators can directly harvest energies from environment and permit flexible manipulation without coupling any external energy-supply systems [8–10]. According to this general principle, bilayer actuators that are responsive to different stimuli, including light [11,12], temperature [13,14], pH value [15,16], solvents [17,18], and moisture [19–21], have been successfully developed based on a wide range of functional materials [22,23], such as polymers [9,24–27], metals [28,29], carbons [12,19–21,30], metal oxides [11,14,31], and even biomaterials [11,14,31].

Among these aforementioned functional materials, typical 2D materials, graphene and its derivatives, have been considered as appealing candidates for developing soft actuators due to their extraordinary physical/chemical properties and sensitive response to different environmental stimuli [17,30,32–34]. For example, taking advantage of the strong interaction between graphene oxide (GO) and water molecules, our group and others have reported the moisture responsive actuators based on GO/reduced GO (RGO) [19–21], multiwall carbon nanotube (MWCNT)/GO [35], and GO-PDA/RGO [36] bilayer structures. Interestingly, all of these actuators consist of two functional layers, a positive material layer that can swell or shrink under external stimuli and a negative layer that is inert to environment changes. Taking the GO/RGO bilayer as an example, the GO layer that has plenty of oxygen containing groups (OCGs) is very sensitive to humidity, it swells in moisture due to the adsorption of water molecules, whereas the RGO layer shows poor water adsorption capability due to the relatively weak interaction with

* Corresponding author.
** Corresponding author.
E-mail addresses: handongdong@jlu.edu.cn (D.-D. Han), hbsun@tsinghua.edu.cn (H.-B. Sun).

https://doi.org/10.1016/j.nanoen.2019.104302
Received 23 September 2019; Received in revised form 31 October 2019; Accepted 14 November 2019
Available online 18 November 2019

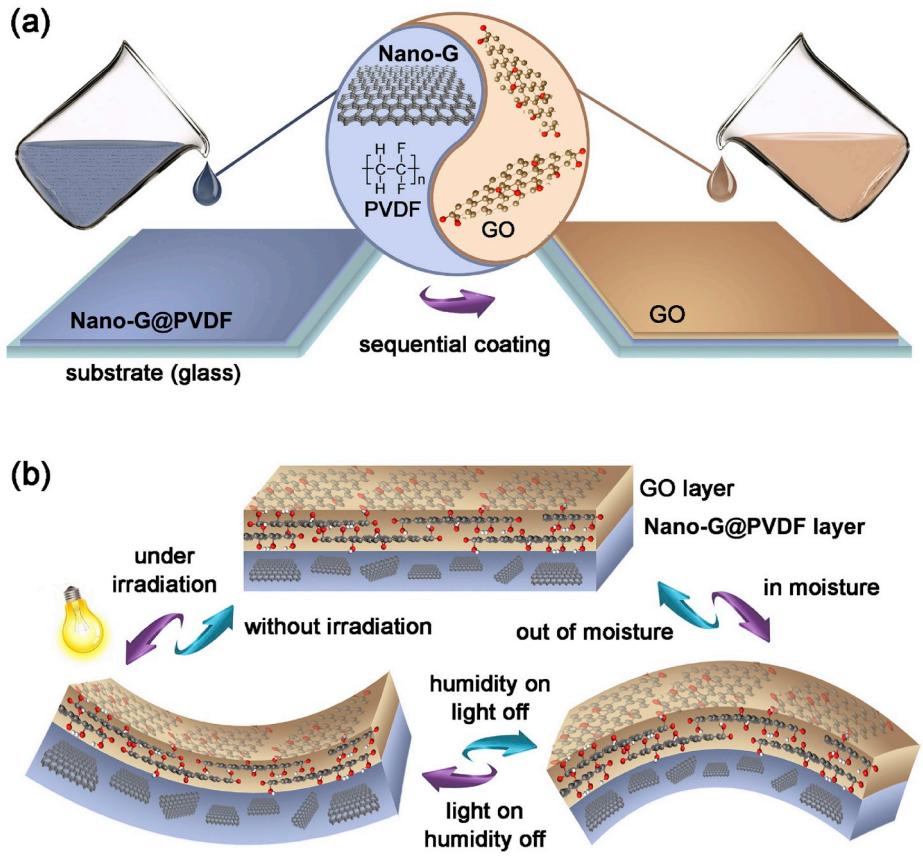

Fig. 1. Design principle of "Yin"-"Yang" complementarity strategy. (a) Schematic illustration of the fabrication process of Nano-G@PVDF/GO bilayer film. (b) The schematic diagram of light and humidity actuation of the Nano-G@PVDF/GO bilayer.

water molecules [37–40]. In this case, the RGO layer is actually not the only choice. Other materials that is not sensitive to moisture is also workable for this kind of moisture actuators. Rational design of bilayer actuators requires maximizing the functionalities of both the positive and negative layers, synchronously. Especially, in the development of dual-responsive or multi-responsive actuators, it is necessary to make full use of the two layers to simplify the actuator structures, instead of simply integrating two or more bilayer devices. However, currently, it still lacks universal concepts to reach this end.

"Yin"-"Yang", the two opposing principles in nature, is a classical theory in the history of Chinese philosophy [41–45]. "Yin" means feminine and negative, and "Yang" indicates masculine and positive. The concept of the complement of "Yin" and "Yang" means that all the things in the world are interdependent and inter-constraint as well as being complementary and relative in "Yin"-"Yang". Actually, this philosophical concept is also applicable worldwide in modern science. In different disciplines, "Yin" and "Yang" may have different scientific meanings, for instance, the binary cooperative complementarity in material science [46], the protons and electrons in physics [47], the Yin deficiency and Yang deficiency in traditional Chinese medicine [48,49], the distinct wettability in surface/interface science [50], as well as neuro-protection and -degeneration in neurochemistry [51]. In this work, we reported the design and fabrication of dual-responsive actuators that enable bi-directional bending according to the basic idea of classical "Yin"-"Yang" complementarity. Here, the complement of "Yin" and "Yang" refers to the distinct response of the two layers under two different stimuli, in which the two layers are interdependent, inter-constraint and complementary for dual-responsive actuation. As a proof-of-concept, composite layer of nano-size graphite (Nano-G) and polyvinylidene fluoride (PVDF) has been combined with GO, forming a bilayer structure. In response to moisture, GO is a positive layer, meaning "Yang", whereas Nano-G@PVDF is a negative layer, meaning "Yin". On the contrary, under light irradiation, GO that has very small coefficient of thermal expansion (CTE) is negative; whereas Nano-G@PVDF layer is positive, since it is photothermally active and has a relatively large CTE. The two layers are "Yin"-"Yang" complemental for moisture and photothermal actuation. In this way, we demonstrated bi-directional walking robot and a smart claw array for controllable moisture and light manipulation. The "Yin"-"Yang" complementarity strategy is a universal concept for designing and fabricating multi-responsive bilayers, holding great promise for developing smart actuating devices.

2. Experiments

2.1. Preparation of Nano-G@PVDF/GO bilayer film

GO was prepared by Hummers' method using natural graphite as raw material. For the preparation of Nano-G, 17 mg of Nano-G and 0.6 ml of N-Methyl pyrrolidone (NMP) solution were mixed and exfoliated by ultrasonic treatment for 24 h. Then, 300 mg of PVDF and 2.4 ml of N, N-Dimethylformamide (DMF) were mixed together under ultrasonic treatment for 2 min. After that, the Nano-G and PVDF solution were mixed together (the weight ratio of Nano-G and PVDF is ~1:18). The mixture was dropped on a glass substrate. After the evaporation of the solvents, a Nano-G@PVDF composite film formed. GO solutions was dropped on the Nano-G@PVDF and dried in a vacuum oven at room temperature.

2.2. Preparation of bi-directional walking robot and smart claw array

The bi-directional walking robot consists of eight Nano-G@PVDF/

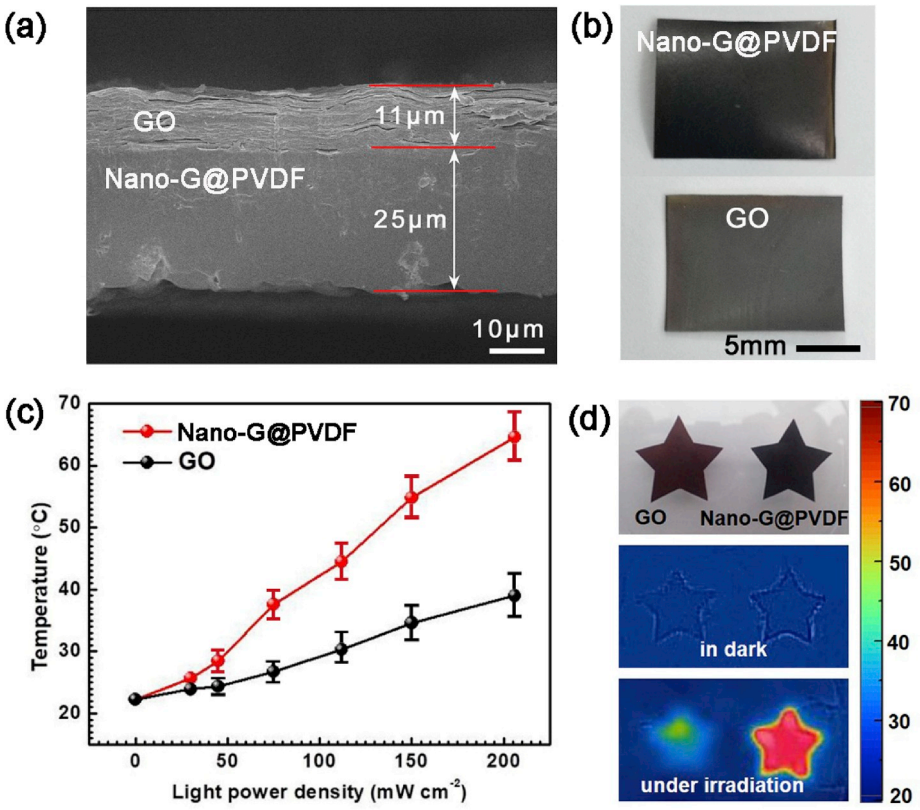

Fig. 2. Morphology and photothermal property. (a) SEM image of the section of a GO and Nano-G@PVDF bilayer film. (b) Photographs of the front and back surface of the bilayer film. (c) Dependence of the local temperature of Nano-G@PVDF and pure GO film on light power density from 0 to 206 mW/cm^2. (d) Photographs and thermography image of GO and Nano-G@PVDF film with and without light irradiation (@206 mW/cm^2).

GO bilayer strips (length, 12 mm; width, 1 mm) working as legs and a square-shaped paper (3.5 mm × 3.5 mm) acting as the main body. The bilayer strips were stuck on the square-shaped paper. Among the four pairs of legs, two pairs opposite to each other use GO as the front side and the other two pairs use Nano-G@PVDF as the front side. The smart claw array was prepared by sticking Nano-G@PVDF/GO bilayer strips (length, ~12 mm; width, 1 mm) on the wall of three plastic tubes. The Nano-G@PVDF/GO bilayer strips were opposite to each other by using GO as outer side and Nano-G@PVDF as inner side.

2.3. Characterization

SEM images were obtained using a JEOL JSM7500 field-emission scanning electron microscope (FE-SEM). FLIR infrared thermal camera (FLIR One) was used to take thermal images. XPS was performed using an ESCALAB 250 spectrometer. XRD pattern was collected on a Rigaku D/MAX 2550 diffractometer with Cu Kα radiation (λ = 1.5418 Å). Humidity environments were obtained *via* saturated aqueous solutions of CH_3COOK, $MgCl_2$, K_2CO_3, NaBr, NaCl, KCl, and K_2SO_4 in a closed glass vessel, which yielded ≈23%, 33%, 44%, 57%, 75%, 86%, and 97% relative humidity (RH), respectively.

3. Results and discussion

3.1. "Yin"-"Yang" complementarity strategy for actuator design

To demonstrate the basic concept of "Yin"-"Yang" complementarity for developing dual-response actuators, we prepared a bilayer film that consists of a layer of Nano-G@PVDF composite and a layer of GO. The preparation procedure is quite simple. As shown in Fig. 1a, Nano-G prepared by solvent exfoliation of nano-size graphite was mixed with PVDF (DMF solution), which is used as a hybrid material for preparing the bottom layer (Nano-G@PVDF). With the help of solvent exfoliation, the Nano-G can be exfoliated into thin layers (Figs. S1 and S2), which can facilitate their dispersion in PVDF. Then, an aqueous solution of GO was casted on the top of the Nano-G@PVDF layer and dried to form the bilayer film. The thickness of GO and Nano-G@PVDF is 11 and 25 μm, respectively (Fig. 2a). It is worthy pointing out that the thicknesses of the two layers are optimized parameters. Actually, both the thicknesses of GO and Nano-G@PVDF layers can affect the deformation properties. For moisture actuation, GO layer is the active layer that drives the deformation, and the Nano-G@PVDF is inert. To reduce the resistance, the Nano-G@PVDF layer should be thinner. On the contrary, under light actuation, the photothermal Nano-G@PVDF layer is the driving layer. It should be thick enough to gain relative larger bending force. To achieve dual-responsive deformation, the two layers should have suitable thicknesses. Nevertheless, the thicknesses are not unalterable. For different applications, their thickness can be further optimized. Here, the "Yin"-"Yang" complementarity concept lies in that Nano-G@PVDF layer can functionalize as a positive layer enabling photothermal expanding, since the carbon doped PVDF film features both high light absorption capability and large CTE (~230 ppm K^{-1}) [52]. Meanwhile, it can also work as negative layer under the actuation of moisture due to the poor water adsorption capability. Therefore, it is necessary to make effective trade-offs about the thickness of Nano-G@PVDF layer. Thicker Nano-G@PVDF layer would generate relative larger driving force under photothermal actuation, and also much larger resistance under moisture actuation. As compared with the Nano-G@PVDF layer, GO layer is totally complementary. With abundant of oxygen containing groups, GO is very sensitive to humidity, it swells obviously in moisture due to the adsorption of water molecules, whereas, considering its relative small CTE (0.85 ppm K^{-1}), GO is inert to temperature change. In this way, a "Yin"-"Yang" complementarity bilayer actuator that is responsive to both light and moisture can be developed. As shown in Fig. 1b, under

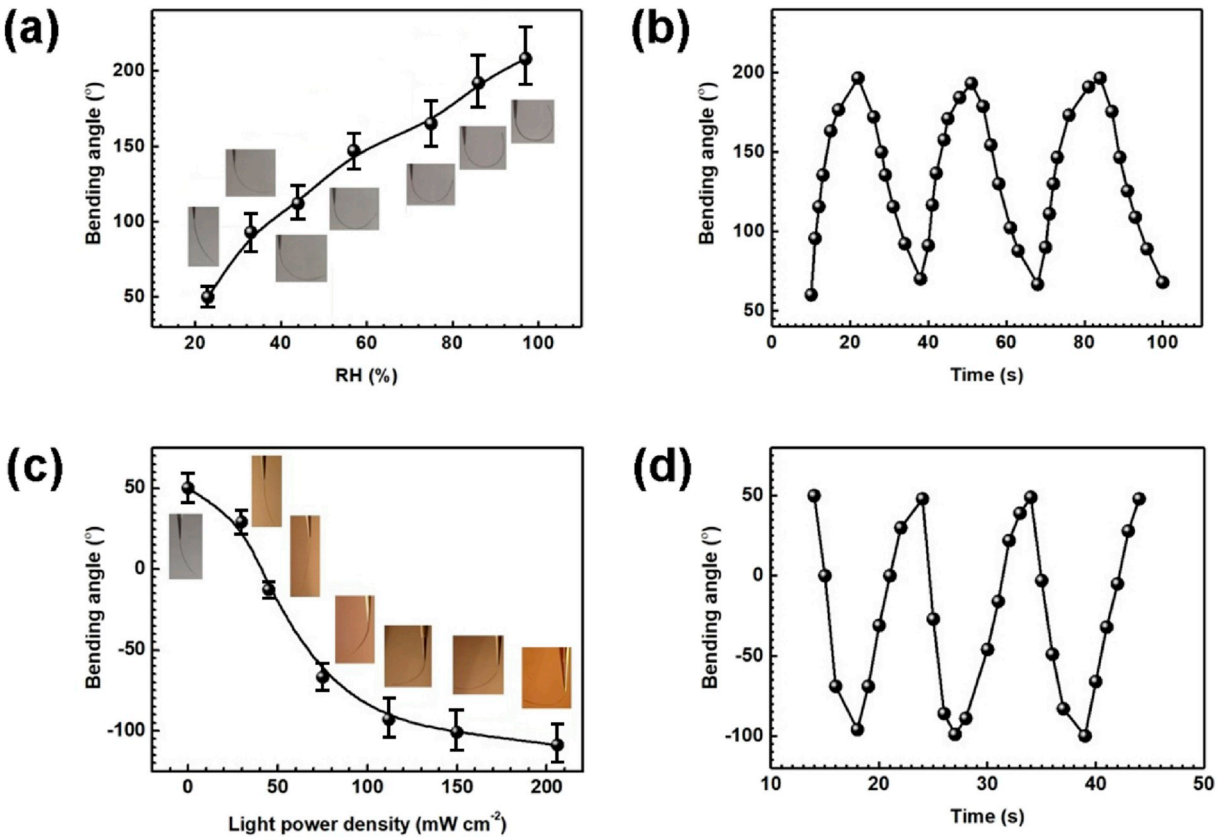

Fig. 3. Moisture and light dual-response properties. (a) Dependence of bending angles of the Nano-G@PVDF/GO bilayer film on RH. The insets are photographs of bending Nano-G@PVDF/GO ribbons under different humidity. (b) The response and recovery curves of Nano-G@PVDF/GO bilayer film between RH = 23% and RH = 97%. (c) Bending angles curves for Nano-G@PVDF/GO bilayer film under light irradiation. The insets are photographs of Nano-G@PVDF/GO ribbons under different light power density. (d) The response and recovery curves of Nano-G@PVDF/GO bilayer film between 0 and 206 mW/cm^2.

light irradiation, the Nano-G@PVDF layer is positive, it tends to expand, whereas GO is negative. The negative effect can be further promoted since the photothermal effect induces water desorption in GO films, leading to the shrinking of the layer. Under moisture actuation, the situation is conversed. GO is positive and Nano-G@PVDF is negative. Since both light irradiation and moisture actuations can lead to an obvious strain mismatch at the bilayer interface, the bilayer actuator is dual-responsive to light and moisture. This "Yin"-"Yang" complementarity is not only suitable for the graphene-based moisture and light dual-responsive actuators. It is a universal strategy and can be applied to different systems.

3.2. Photothermal property

To better understand the photothermal conversion ability of the Nano-G@PVDF layer, we tested its surface temperatures under light irradiation at different light power density and compared with that of GO film (Fig. 2b and c). Notably, Nano-G@PVDF film shows much better photothermal effect than GO film. As the light power density increased from 0 to 206 mW/cm^2, the surface temperature of Nano-G@PVDF gradually increased from room temperature (22.2 °C) to 64.6 °C. On the contrary, when strong light (power density of 206 mW/cm^2) irradiates GO, the surface temperature is only ~39 °C. The slope of the curve, denoted as the photothermal sensitivity, is calculated to be ~0.08 °C per mW/cm^2 for GO; whereas the sensitivity of Nano-G@PVDF is ~0.21 °C per mW/cm^2, 2.6 times of GO. To make a direct comparison of the photothermal effect between these two layers, thermography images have been taken under strong light irradiation (206 mW/cm^2). As shown in Fig. 2d, the Nano-G@PVDF film exhibits much higher temperature distribution than the GO film, indicating the remarkable photothermal conversion ability of the Nano-G@PVDF film. In addition to the difference in photothermal effect, we should also notice that GO and PVDF have distinct CTE (GO, 0.85 ppm K^{-1}, PVDF, ~230 ppm K^{-1}, Nano-G, −1 and 29 ppm K^{-1} along different direction) [52–56], and the CTE of PVDF is much larger than that of GO. In this case, the photothermal expanding of the Nano-G@PVDF layer would be more obvious than that of GO upon light actuation.

3.3. Light and moisture responsive property

For moisture responsive property, Nano-G@PVDF layer is undoubtedly a negative layer since both graphite and PVDF shows relative weak interaction with water molecules. However, for GO, the situation is different. FTIR spectrum of GO (Fig. S3) confirmed that there exists plenty of OCGs on the GO streets. The XPS results are consistent with FTIR, carbon-to-oxygen atom ratio (C/O) is as low as 2.17, indicating the high oxygen content (Fig. S4). The XRD pattern of GO shows that the *d*-spacing between GO nanosheets is 7.6 Å (Fig. S5), this value further depends on the amount of water adsorbed by GO. Due to the presence of abundant OCGs on GO nanosheets, water molecules would interact with GO by forming hydrogen bonds. In this case, water molecules could be selectively adsorbed by GO, leading to obvious expansion of GO layer under moisture actuation.

We further test the moisture responsive property of the bilayer actuators. As a positive layer for moisture actuation, the Nano-G@PVDF/GO bilayer bends towards the Nano-G@PVDF side when exposed to moisture. Moisture responsiveness under different RH is shown in Fig. 3a. The bending angle of the bilayer actuator (2 cm*0.1 cm) increases from 50° to 208° when the ambient moisture increased from RH = 23% to RH = 97%. The initial bending angle (50°) of the bilayer

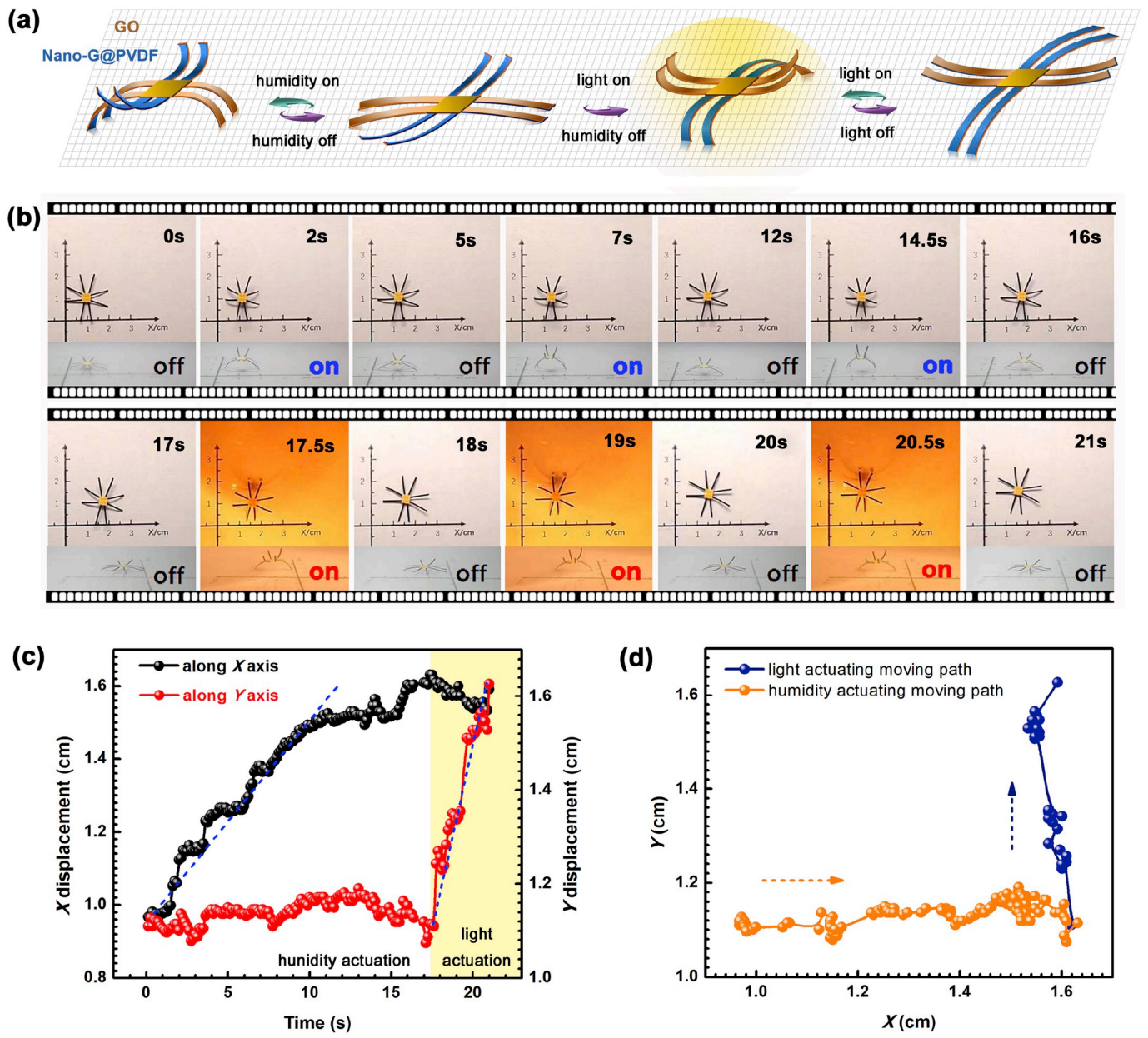

Fig. 4. Dual-responsive bi-directional walking robot. (a) Schematic illustration of moisture/light dual-responsive bi-directional walking robot. (b) The bi-directional walking robot moves along the *x* direction in response to the humidity and moves along the *y* direction in response to light irradiation. (c) The *x*-axis displacement and *y*-axis displacement of the bi-directional walking robot at different time. (d) The path of bi-directional walking robot under humidity and light actuation.

ribbon is due to the 23% RH at the ambient condition. Herein, the bending curvature, can be described as follows (see Fig. S6) [22,57–59]:

$$k \propto (\beta_2 - \beta_1)\Delta RH$$

where k is the bending curvature of the actuator, β_1 and β_2 are the respective coefficient of hygroscopic expansion (CHE) for Nano-G@PVDF and GO, respectively. ΔRH is the relative humidity change. Besides, the moisture induced deformation is reversible. When the ribbon was exposed to dry air, it recovered to its original shape after desorption of water. In this way, a reversible bending/unbending deformation can be achieved by moisture actuation. The response time is measured to be ~13 s and the recovery time is ~16 s, when the ambient humidity was switched between RH = 23% and RH = 97% (Fig. 3b).

Owing to the different photothermal activity, the Nano-G@PVDF layer with broad-spectrum absorption capability and relatively larger CTE is positive. It can convert the photon energy into heat effectively under light irradiation, which caused the expansion of the Nano-G@PVDF layer. On the contrary, the GO layer is negative. Notably, GO has very small CTE. With the increase of local temperature, GO layer even shrinks due to the thermal effect induced desorption of water. In this regard, both the photothermal expansion of the Nano-G@PVDF layer and the photothermal desorption of GO would induce the strain mismatch between the two layers (see Fig. S7) [22,57–59]. The bending curvature, can be described as follows:

$$k \propto (\alpha_1 - \alpha_2)\Delta T + \beta_2 \Delta C_2$$

where k is the bending curvature of the actuator, α_1 and α_2 are the respective CTE for layers Nano-G@PVDF and GO, ΔT is the photoinduced temperature change, β_2 is the respective CHE of layer GO materials, and ΔC_2 is the change of moisture concentration in layers GO due to the photothermal effect, respectively.

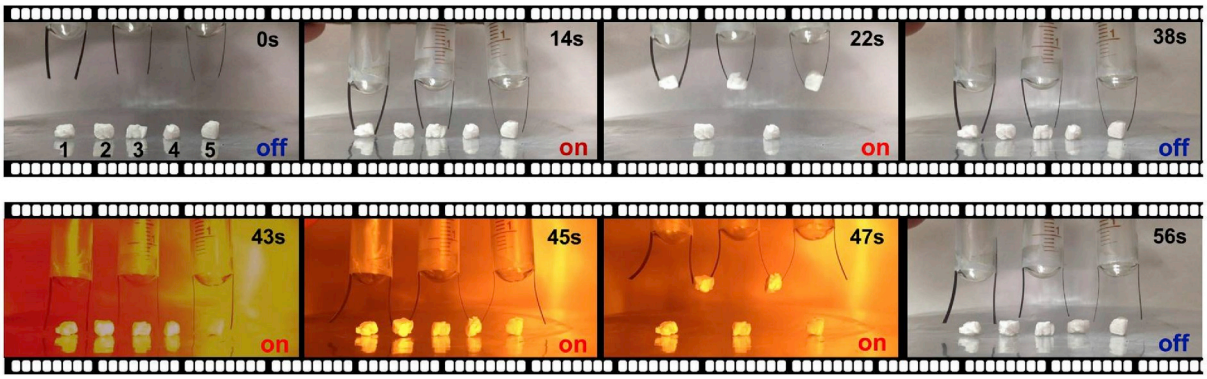

Fig. 5. Dual-responsive smart claw array. Light and moisture manipulation of the smart claw array. Under moisture actuation, Nano-G@PVDF/GO bilayer ribbons bend to the Nano-G@PVDF side, lifting the polymer foams No.1, 3 and 5. Under light irradiation, the claw array releases these polymer foams and lifts the polymer foams No. 2 and 4.

Under light irradiation, the bilayer ribbon bends to the GO side from 50° to −109° with the increase of light intensity (Fig. 3c). The light actuation is also reversible. Without light irradiation, the Nano-G@PVDF/GO bilayer film can recover to initial bending angle gradually. As compared with moisture actuation, the response under light irradiation is much faster. We recorded the deformation process of the Nano-G@PVDF/GO bilayer film by switching the light intensity between 0 and 206 mW/cm^2. As shown in Fig. 3d, the response time is ~4 s and the recovery time is ~6 s. To further investigate the photothermal effect induced bending process, we also tested the relationship between temperature and bending angles (Fig. S8). In addition, the Nano-G@PVDF/GO bilayer actuator shows good stability and durability under moisture and light actuation. The bilayer is stable under both moisture and light actuation. The actuator shows good durability in 100 times of actuation (Fig. S9.) Moreover, the two layers show tight interfacial contact before and after frequent actuation for 100 times, indicating the good interlayer adhesion (Fig. S10).

3.4. Bi-directional walking robot

Taking advantage of the moisture and light dual-responsive property, we designed and fabricated two typical actuators using the Nano-G@PVDF and GO bilayer film (Video S1). As a proof of concept, we first demonstrated the light and moisture dual-responsive walking robot that enables bi-directional walking under light and moisture stimulation. Fig. 4a shows the schematic illustration of the device structure and its working principle. Briefly, it consists of eight Nano-G@PVDF/GO bilayer strips working as legs and a square-shaped paper acting as main body. To keep a balance during walking, a pair of legs has been integrated with each side of the square body. Among the four pairs of legs, two pairs oppositing to each other use GO as front side and the other two pairs use Nano-G@PVDF as front side. In this way, the robot can walk along different direction under light and moisture actuation. The detailed scheme for the moisture supplying system for this walking robot is shown in Fig. S11. When the robot was exposed to moisture (RH ~ 100%), the Nano-G@PVDF/GO bilayer legs bend toward the Nano-G@PVDF side. In this case, the legs with GO as front side bend downwards, whereas the legs with Nano-G@PVDF as front side bend upwards. By switching the environmental humidity, the legs bend downside and recover alternately, leading the moving toward the *x* axis direction (Fig. 4b). When we keep the environmental humidity constant, light irradiation can trigger the downwards bending of legs with Nano-G@PVDF as front side and the upwards bending of the other two pairs of legs. The walking robot were exposed to the filament light (~100 W) with a distance of 20 cm. Upon alternative light stimulation, the robot moves along the *y* axis direction (Fig. 4b). Actually, the humidity or light can only cause simple bending and unbending deformation of the bilayer ribbons (legs). To realize directional walking, we drive the "walking robot" through the humidity and the light gradient. As shown in Fig. S12, in humidity actuation, the moisture is supplied from the left side of the "walking robot". In this way, a localized humidity gradient formed around the "walking robot". Its left legs bent to larger degree and earlier than the right legs, so the robot moved towards the right side. Under light actuation, the light irradiated from the bottom side, thus the legs near the light source bent to larger degree than the other two legs. In this way, it moved upside.

Supplementary video related to this article can be found at https://doi.org/10.1016/j.nanoen.2019.104302.

We further analyzed the process of both moisture and light actuation of the robot and recorded the displacement along *x* and *y* axes, respectively. As shown in Fig. 4c, under moisture actuation, the robot moved ~0.6 cm along the *x* axis in 15s, whereas under light actuation, it moved 0.5 cm in 5s. The average moving speeds are calculated to be 0.4 mm/s and 1 mm/s for moisture and light actuation, respectively. The difference in moving speed under moisture and light actuation can be attributed to the on/off frequency of the stimuli and the response/recovery time of the bilayer under different stimuli. Fig. 4d shows the moving track of the robot under humidity/light actuation.

3.5. Dual-responsive smart claw array

Since the Nano-G@PVDF/GO bilayer strips can bend toward different direction under moisture and light actuation, we designed and fabricated a smart claw array (Video S2). In this device, we integrated 6 Nano-G@PVDF/GO bilayer strips together, connecting to three plastic tubes that can supply moisture. The strips on the left of the plastic tubes used GO as left side and Nano-G@PVDF as right side, whereas the other strips used the opposite side of the bilayer. Fig. 5 shows the manipulation of this smart claw array for selectively picking up polymer foam blocks using moisture and light actuation, respectively. Interestingly, when the claw is exposed to moisture, all of the stripes bend toward the Nano-G@PVDF sides. In this way, the claw array picks up the No.1, 3 and 5 polymer foam blocks. Under light stimulation (filament light, ~100 W; distance, 20 cm), the strips bend to the GO side, and the claw array lift the No. 2, 4 polymer foam blocks, realizing the selectively picking up function.

Supplementary video related to this article can be found at https://doi.org/10.1016/j.nanoen.2019.104302.

4. Conclusions

In conclusion, the concept of Yin-Yang complementarity has been adopted for design and fabrication of dual-responsive bimorph actuators. The essence of the Yin-Yang complementarity strategy lies in the

development of bilayer structures, in which one layer is positive to a certain stimulus but negative to another; whereas the other layer shows complementary response to the two stimuli. According to this principle, dual-responsive actuators, such as bilayer structures of Nano-G@PVDF/GO, have been successfully prepared to verify this concept and the dual-responsive property (Table S1). As a proof-of-concept, Nano-G@PVDF/GO bilayer has been employed for fabricating light and moisture dual-responsive actuators, in which bi-directional walking robot and smart claw array demonstrated controllable and predictable deformation under the synergetic actuation. Unlike those GO- or PVDF-based bilayer actuators that consist of an active layer and an inert layer. We make full use of the two layers. They are completely complementary under moisture/light actuation. In addition, the complementary design principle is universal for actuators design. We deem that it can be applicable for many types of soft, wet and smart systems in the future [60,61]. As a universal design principle, the Yin-Yang complementarity strategy provides a general method for developing multi-responsive bimorph actuators in the simplest way.

Declaration of competing interest

The authors declare that they have no known competing financial interests or personal relationships that could have appeared to influence the work reported in this paper.

Acknowledgements

This work was supported by the National Key Research and Development Program of China and National Natural Science Foundation of China (NSFC) under Grant Nos. #2017YFB1104300, #61935008, #61590930, #61775078 and #61905087. Scientific and Technological Developing Scheme of Jilin Province Nos. #20180101061JC.

Appendix A. Supplementary data

Supplementary data to this article can be found online at https://doi.org/10.1016/j.nanoen.2019.104302.

References

[1] D.D. Han, Y.L. Zhang, J.N. Ma, Y.Q. Liu, B. Han, H.B. Sun, Light-mediated manufacture and manipulation of actuators, Adv. Mater. 28 (2016) 8328.
[2] J.N. Wang, Y.Q. Liu, Y.L. Zhang, J. Feng, H. Wang, Y.H. Yu, H.B. Sun, Wearable superhydrophobic elastomer skin with switchable wettability, Adv. Funct. Mater. 28 (2018) 1800625.
[3] S. Juodkazis, MANUFACTURING 3D printed micro-optics, Nat. Photonics 10 (2016) 499.
[4] Q. Li, Intelligent Stimuli-Responsive Materials: from Well-Defined Nanostructures to Applications, John Wiley & Sons, 2013.
[5] Q. Zhao, Y.H. Liang, L. Ren, Z.L. Yu, Z.H. Zhang, L.Q. Ren, Bionic intelligent hydrogel actuators with multimodal deformation and locomotion, Nano Energy 51 (2018) 621.
[6] M.S. Noh, H. Lee, Y.G. Song, I. Jung, R. Ning, S.W. Paek, H.C. Song, S.H. Baek, C. Y. Kang, S. Kim, Li alloy-based non-volatile actuators, Nano Energy 57 (2019) 653.
[7] L.L. Wang, J.A. Jackman, E.L. Tan, J.H. Park, M.G. Potroz, E.T. Hwang, N.J. Cho, High-performance, flexible electronic skin sensor incorporating natural microcapsule actuators, Nano Energy 36 (2017) 38.
[8] J. Shintake, V. Cacucciolo, D. Floreano, H. Shea, Soft robotic grippers, Adv. Mater. 30 (2018) 1707035.
[9] G. Wang, H. Xia, X.C. Sun, C. Lv, S.X. Li, B. Han, Q. Guo, Q. Shi, Y.S. Wang, H. B. Sun, Actuator and generator based on moisture-responsive PEDOT: PSS/PVDF composite film, Sens. Actuators B Chem. 255 (2017) 1415.
[10] Z.K. Yuan, X.F. Xiao, J. Li, Z. Zhao, D.S. Yu, Q. Li, Self-assembled graphene-based architectures and their applications, Adv. Sci. 5 (2018) 1700626.
[11] T. Wang, D. Torres, F.E. Fernandez, C. Wang, N. Sepulveda, Maximizing the performance of photothermal actuators by combining smart materials with supplementary advantages, Sci. Adv. 3 (2017) 1700626.
[12] M. Amjadi, M. Sitti, Self-sensing paper actuators based on graphite-carbon nanotube hybrid films, Adv. Sci. 5 (2018) 1800239.
[13] G.C. Xu, M. Zhang, Q.Q. Zhou, H.W. Chen, T.T. Gao, C. Li, G.Q. Shi, A small graphene oxide sheet/polyvinylidene fluoride bilayer actuator with large and rapid responses to multiple stimuli, Nanoscale 9 (2017) 17465.
[14] H.K. Bisoyi, A.M. Urbas, Q. Li, Soft materials driven by photothermal effect and their applications, Adv. Opt. Mater. 6 (2018) 1800458.
[15] C.X. Ma, W. Lu, X.X. Yang, J. He, X.X. Le, L. Wang, J.W. Zhang, M.J. Serpe, Y. J. Huang, T. Chen, Bioinspired anisotropic hydrogel actuators with on-off switchable and color-tunable fluorescence behaviors, Adv. Funct. Mater. 28 (2018) 1704568.
[16] Y.W. Hu, J.S. Kahn, W.W. Guo, F.J. Huang, M. Fadeev, D. Harries, I. Willner, Reversible modulation of DNA-based hydrogel shapes by internal stress interactions, J. Am. Chem. Soc. 138 (2016) 16112.
[17] T. Deng, C. Yoon, Q.R. Jin, M.G. Li, Z.W. Liu, D.H. Gracias, Self-folding graphene-polymer bilayers, Appl. Phys. Lett. 106 (2015) 203108.
[18] J. Bai, Z.X. Shi, J. Yin, M. Tian, R.J. Qu, Shape reconfiguration of a biomimetic elastic membrane with a switchable janus structure, Adv. Funct. Mater. 28 (2018) 1800939.
[19] D.D. Han, Y.L. Zhang, Y. Liu, Y.Q. Liu, H.B. Jiang, B. Han, X.Y. Fu, H. Ding, H.L. Xu, H.B. Sun, Bioinspired graphene actuators prepared by unilateral UV irradiation of graphene oxide papers, Adv. Funct. Mater. 25 (2015) 4548.
[20] D.D. Han, Y.L. Zhang, H.B. Jiang, H. Xia, J. Feng, Q.D. Chen, H.L. Xu, H.B. Sun, Moisture-responsive graphene paper prepared by self-controlled photoreduction, Adv. Mater. 27 (2015) 332.
[21] H.H. Cheng, J. Liu, Y. Zhao, C.G. Hu, Z.P. Zhang, N. Chen, L. Jiang, L.T. Qu, Graphene fibers with predetermined deformation as moisture-triggered actuators and robots, Angew. Chem. Int. Ed. 52 (2013) 10482.
[22] M. Amjadi, M. Sitti, High-performance multiresponsive paper actuators, ACS Nano 10 (2016) 10202.
[23] L. Gao, G.Q. Guo, M.J. Liu, Z.G. Tang, L.X. Xie, Y.P. Huo, Multi-responsive, bidirectional, and large deformation bending actuators based on borax cross-linked polyvinyl alcohol derivative hydrogel, RSC Adv. 7 (2017) 40005.
[24] H. Lim, T. Park, J. Na, C. Park, B. Kim, E. Kim, Construction of a photothermal Venus flytrap from conductive polymer bimorphs, NPG Asia Mater. 9 (2017) e399.
[25] D.H. Gracias, Stimuli responsive self-folding using thin polymer films, Curr. Opin. Chem. Eng. 2 (2013) 112.
[26] X. Li, X.B. Cai, Y.F. Gao, M.J. Serpe, Reversible bidirectional bending of hydrogel-based bilayer actuators, J. Mater. Chem. B 5 (2017) 2804.
[27] M.C. Weng, P.D. Zhou, L.Z. Chen, L.L. Zhang, W. Zhang, Z.G. Huang, C.H. Liu, S. S. Fan, Multiresponsive bidirectional bending actuators fabricated by a pencil-on-paper method, Adv. Funct. Mater. 26 (2016) 7244.
[28] B.R. Xu, Z. Tian, J. Wang, H. Han, T. Lee, Y.F. Mei, Stimuli-responsive and on-chip nanomembrane micro-rolls for enhanced macroscopic visual hydrogen detection, Sci. Adv. 4 (2018), eaap8203.
[29] F. Qiu, S. Fujita, R. Mhanna, L. Zhang, B.R. Simona, B.J. Nelson, Magnetic Helical microswimmers functionalized with lipoplexes for targeted gene delivery, Adv. Funct. Mater. 25 (2015) 1666.
[30] C. Luo, C.N. Yeh, J.M.L. Baltazar, C.L. Tsai, J.X. Huang, A cut-and-paste approach to 3D graphene-oxide-based architectures, Adv. Mater. 30 (2018) 1706229.
[31] F. Feng, W.Y. Yang, S. Gao, L.G. Zhu, Q. Li, Photoinduced reversible lattice expansion in W-doped TiO_2 through the change of its electronic structure, Appl. Phys. Lett. 112 (2018), 061904.
[32] P. Kang, K.H. Kim, H.G. Park, S. Nam, Mechanically reconfigurable architectured graphene for tunable plasmonic resonances, Light Sci. Appl. 7 (2018) 17.
[33] X.W. Yu, H.H. Cheng, M. Zhang, Y. Zhao, L.T. Qu, G.Q. Shi, Graphene-based smart materials, Nat. Rev. Mater. 2 (2017) 17046.
[34] L. Wang, H.K. Bisoyi, Z.G. Zheng, K.G. Gutierrez-Cuevas, G. Singh, S. Kumar, T. J. Bunning, Q. Li, Stimuli-directed self-organized chiral superstructures for adaptive windows enabled by mesogen-functionalized graphene, Mater. Today 20 (2017) 230.
[35] J. Mu, C. Hou, H. Wang, Y. Li, Q. Zhang, M. Zhu, Origami-inspired active graphene-based paper for programmable instant self-folding walking devices, Sci. Adv. 1 (2015), e1500533.
[36] M.Y. Ji, N. Jiang, J. Chang, J.Q. Sun, Near-infrared light-driven, highly efficient bilayer actuators based on polydopamine-modified reduced graphene oxide, Adv. Funct. Mater. 24 (2014) 5412.
[37] Y.J. Li, T.T. Gao, Z. Yang, C.J. Chen, Y.D. Kuang, J.W. Song, C. Jia, E.M. Hitz, B. Yang, L.B. Hu, Graphene oxide-based evaporator with one-dimensional water transport enabling high-efficiency solar desalination, Nano Energy 41 (2017) 201.
[38] H.H. Cheng, Y.X. Huang, L.T. Qu, Q.L. Cheng, G.Q. Shi, L. Jiang, Flexible in-plane graphene oxide moisture-electric converter for touchless interactive panel, Nano Energy 45 (2018) 37.
[39] C.X. Shao, J. Gao, T. Xu, B.X. Ji, Y.K. Xiao, C. Gao, Y. Zhao, L.T. Qu, Wearable fiberform hygroelectric generator, Nano Energy 53 (2018) 698.
[40] R. You, Y.Q. Liu, Y.L. Hao, D.D. Han, Y.L. Zhang, Z. You, Laser fabrication of graphene-based flexible electronics, Adv. Mater. (2019), https://doi.org/10.1002/adma.201901981.
[41] Y. Shaked, Balancing efficacy of and host immune responses to cancer therapy: the yin and yang effects, Nat. Rev. Clin. Oncol. 13 (2016) 611.
[42] G. Prieto, F. Schuth, The Yin and Yang in the development of catalytic processes: catalysis research and reaction engineering, Angew. Chem. Int. Ed. 54 (2015) 3222.
[43] M.X. Jiao, L.H. Jing, X.J. Wei, C.Y. Liu, X.L. Luo, M.Y. Gao, The Yin and Yang of coordinating co-solvents in the size-tuning of Fe_3O_4 nanocrystals through flow synthesis, Nanoscale 9 (2017) 18609.
[44] Y. Jin, Y.L. Tan, X.Z. Hu, B. Zhu, Q.H. Zheng, Z.J. Zhang, G.Y. Zhu, Q. Yu, Z. Jin, J. Zhu, Scalable production of the silicon-tin Yin-Yang hybrid structure with graphene coating for high performance lithium-ion battery anodes, ACS Appl. Mater. Interfaces 9 (2017) 15388.
[45] X.D. Tang, L.B. Huang, Y.L. Xu, J.D. Yang, W.Q. Wu, H.F. Jiang, Copper-catalyzed coupling of oxime acetates with sodium sulfinates: an efficient synthesis of sulfone derivatives, Angew. Chem. Int. Ed. 53 (2014) 4205.

[46] R.C. Fang, M.J. Liu, L. Jiang, Progress of binary cooperative complementary interfacial nanomaterials, Nano Today 24 (2019) 48.
[47] J.L. Xia, L. Jiang, Dialectics of nature: temporal and spatial regulation in material sciences, Nano Res. 10 (2017) 1115.
[48] Q.N. Hu, T. Yu, J.H. Li, Q. Yu, L. Zhu, Y.G. Gu, End-to-end syndrome differentiation of Yin deficiency and Yang deficiency in traditional Chinese medicine, Comput. Methods Progr. Biomed. 174 (2019) 9.
[49] T.N. Zhao, H.J. Wang, C.Q. Yu, J. Wang, Y.W. Cui, X. Zheng, B. Wang, W.J. Wang, J.Y. Meng, Classification and differentiation between kidney yang and yin decficiency syndromes in TCM based on decision tree analysis method, Int. J. Clin. Exp. Med. 9 (2016) 21888.
[50] R.C. Fang, M.J. Liu, H.L. Liu, L. Jiang, Bioinspired interfacial materials: from binary cooperative complementary interfaces to superwettability systems, Adv. Mater. Interfaces 5 (2018) 1701176.
[51] J.J. Alexander, A.J. Anderson, S.R. Barnum, B. Stevens, A.J. Tenner, The complement cascade: Yin-Yang in neuroinflammation - neuro-protection and -degeneration, J. Neurochem. 107 (2008) 1169.
[52] B. Wang, H.X. Huang, Incorporation of halloysite nanotubes into PVDF matrix: nucleation of electroactive phase accompany with significant reinforcement and dimensional stability improvement, Compos. Appl. Sci. Manuf. 66 (2014) 16.
[53] J. Zhu, C.M. Andres, J.D. Xu, A. Ramamoorthy, T. Tsotsis, N.A. Kotov, Pseudonegative thermal expansion and the state of water in graphene oxide layered assemblies, ACS Nano 6 (2012) 8357.
[54] L.Z. Chen, M.C. Weng, P.D. Zhou, L.L. Zhang, Z.G. Huang, W. Zhang, Multi-responsive actuators based on a graphene oxide composite: intelligent robot and bioinspired applications, Nanoscale 9 (2017) 9825.
[55] M.S. Asl, M.G. Kakroudi, R.A. Kondolaji, H. Nasiri, Influence of graphite nano-flakes on densification and mechanical properties of hot-pressed ZrB_2-SiC composite, Ceram. Int. 41 (2015) 5843.
[56] R. Prieto, J.M. Molina, J. Narciso, E. Louis, Fabrication and properties of graphite flakes/metal composites for thermal management applications, Scr. Mater. 59 (2008) 11.
[57] H.C. Bi, K.B. Yin, X. Xie, Y.L. Zhou, S. Wan, F. Banhart, L.T. Sun, Microscopic bimetallic actuator based on a bilayer of graphene and graphene oxide, Nanoscale 5 (2013) 9123.
[58] X.N. Zang, Q. Zhou, J.Y. Chang, Y.M. Liu, L.W. Lin, Graphene and carbon nanotube in MEMS/NEMS applications, Microelectron. Eng. 132 (2015) 192.
[59] Z.H. Khan, A.R. Kermany, A. Ochsner, F. Iacopi, Mechanical and electromechanical properties of graphene and their potential application in MEMS, J. Phys. D Appl. Phys. 50 (2017) 24.
[60] M. Nishizawa, Soft, wet and ionic microelectrode systems, Bull. Chem. Soc. Jpn. 91 (2018) 1141.
[61] B. Han, Y.L. Zhang, L. Zhu, Y. Li, Z.C. Ma, Y.Q. Liu, X.L. Zhang, X.W. Cao, Q. D. Chen, C.W. Qiu, H.B. Sun, Plasmonic-assisted graphene oxide artificial muscles, Adv. Mater. 31 (2019) 1806386.

Yong-Lai Zhang received his B.S. (2004) and Ph.D. (2009) from Jilin University, China. He is currently a full professor in the State Key Laboratory of Integrated Optoelectronics, College of Electronic Science and Engineering, Jilin University. In 2011, he was awarded a "Hong Kong Scholar" postdoctoral fellow. His research interests include laser fabrication, graphene-based microdevices, soft robotics and Lab-on-a-Chip systems.

Jia-Nan Ma is currently pursuing her Ph.D. at Jilin University, China. Her research interests include intelligent actuators based on graphene.

Sen Liu is a Master student at Jilin University, China. His research interest has been focused on laser fabrication of graphene devices and applications in actuators.

Dong-Dong Han received his B.S. (2013) and Ph.D. (2018) from College of Electronic Science and Engineering, Jilin University, China. Currently, his research interest is focused on laser fabrication of graphene-based soft robots.

Yu-Qing Liu is pursuing her Ph.D. at Jilin University, China. Her research interests lie in the field of biomimetic fabrication, bio-inspired materials, and bionic devices.

Zhao-Di Chen is currently a Master student at Jilin University, China. Her research interest is functional actuators based on graphene.

Jiang-Wei Mao is currently a Master student at Jilin University, China. Her research interests include functional actuators based on graphene.

Hong-Bo Sun received his B.S. and Ph.D. degrees in electronics from Jilin University, China, in 1992 and 1996, respectively. He worked as a postdoctoral researcher in Satellite Venture Business Laboratory, the University of Tokushima, Japan, from 1996 to 2000, and then as an assistant professor in Department of Applied Physics, Osaka University, Osaka, Japan. In 2005, he was promoted as a full professor (Changjiang Scholar) in Jilin University, China. In 2017, he joined Tsinghua University as a professor. His research interests have been focused on ultrafast optoelectronics, particularly on laser nanofabrication and ultrafast spectroscopy.